

Quantification of the Local Heat Release Rate During Flame-Vortex Interactions at Different Lewis Numbers and Equivalence Ratios

J.A. Denev*, I. Naydenova, and H. Bockhorn

Karlsruhe Institute of Technology, Engler-Bunte-Institute; Engler-Bunte-Ring 1,
76131 Karlsruhe, Germany

Abstract

The present work aims at the detailed understanding of the local processes in premixed combustion of hydrogen, methane and propane flames at unsteady conditions. The methodology consists of the analysis of simulations of two-dimensional flame-vortex interactions as well as statistical data obtained from three-dimensional Direct Numerical Simulations (DNS) of the flame front interacting with a set of vortices. Special attention is given to the relationship between the Lewis number (Le) of the fuel and the flame front stretch in terms of both curvature and strain rate. A large single vortex bends the flame front thus creating both positive and negative curvatures, which in turn enhance the heat release rate in some locations of the flame front and decrease it in others. The resulting effect is called "polarisation effect". The occurrence and the strength of the polarisation effect of curvature are tightly bound up with the Lewis number of the fuel. The polarisation effect is quantified by the ratio of maximum to minimum heat release rates along the flame front, which defines the Polarisation Effect Number (PEN). The more the Lewis number of a fuel deviates from unity, the stronger the polarisation effect is. Strong polarisation effects lead finally to local flame extinction. This is demonstrated for hydrogen flames with $Le = 0.29$ (lean) and $Le = 2.2$ (rich) as well as for artificially designed cases with $Le = 0.1$ and $Le = 10.0$. Therefore, flame extinction can occur for both thermodynamically stable and unstable flames. It is shown that choosing an appropriate mixture of real fuels with different Lewis numbers, the homogeneity of the heat release rate along the flame front could be considerably enhanced. This relatively uniform heat release rate is not sensitive to curvature, which consequently decreases the occurrence of local extinction.

Keywords: Lewis number effect, flame front curvature, tangential strain rate, premixed combustion, local extinction, DNS.

1. Introduction

The influence of the flame front curvature on the intensity of the local processes in premixed combustion has been recognised for long time [1] and since then is widely studied. Williams [2] points out the significance of curvature and strain rate on the local flame structure. Both curvature and aerodynamic tangential strain rate are parts (addends) of the flame stretch [3, 4] defined as the relative increase of the area of the flame front with time.

Asymptotic analysis [2, 5] assumes that, at low stretch values, the flame structure depends only on stretch and that the flame speed is linearly depending on stretch. As described in [6], the asymptotic analysis further assumes that both curvature and

strain play similar roles. Thus a very important simplification is accepted which allows studying the local flame behaviour considering only strained flames. Stationary strained flames can be measured and computed relatively easily with the twin opposite nozzle arrangement. Hence many investigations [e.g. 7, 8, 9, 10 and citations therein] focus on the effects of linear straining on the flame structure and on the flame speed. Main parameters for the obtained results in laminar flames are the strain rate and the equivalence ratio of the gas mixture. The unsteady response of such flames to sinusoidally changing inlet velocities are studied numerically in [11, 12, 13].

When the above-mentioned linear dependence of flame speed on stretch is considered in terms of dimensionless variables, the Markstein number is

* Corresponding author. E-mail: yordan.denev@kit.edu

introduced and this forms the base for the Markstein analysis [14, 15, 16, 17, 18]. Results for the Markstein number (Ma) of laminar non-stretched flames are presented usually as a function of the equivalence ratio with the functional relationship depending on the particular fuel considered. In case of turbulent flames, the Markstein number depends additionally on the characteristics of turbulence. Further, the Markstein number depends also on the temperature of unburnt gases and on the pressure. Therefore, it becomes obvious that a high number of complex experiments or simulations need to be carried out in order to obtain Ma and the corresponding turbulent flame speed. Beside this, in the prevailing part of the turbulent flames the assumption of linear dependence between stretch and flame structure, which is basic for the Markstein analysis, is no longer valid and corresponding corrections are necessary, see e.g. [14, 19].

Laminar flame front stability includes the thermodiffusive properties of the gas mixture and is related to the combined effect of curvature and Lewis number, Le [6, 5, 2]. Therefore, as shown further, many studies focus on the connectivity of curvature and Le of the deficient reactant (fuel or oxidizer), while tangential straining is assumed to be of less importance.

In turbulent premixed flames, there is a strong correlation between the turbulent flame speed and the properties of turbulence such as its length scale and intensity [20, 21, 22]. Therefore, many studies focus on the statistical properties of turbulence and their impact on the flame properties. As a result, another research direction, summarizing the effects of turbulence in regions of combustion diagrams (e.g. the so-called Borghi diagram, [23] and its numerous modifications, [6, 20, 24]) emerges.

Two- or three-dimensional highly resolved numerical simulations can be used to investigate the local physical effects at the flame front interacting with a single vortex or a vortex pair. Since the 1980's [25, 26] such simulations are the forerunners of the Direct Numerical Simulations (DNS) of turbulent flows, which in turn resolve all turbulent vortices. Therefore, the flame-vortex numerical methodology delivers useful detailed information for local processes at the flame front. This methodology forms the main part of the investigation in the present work. In order to supplement the obtained results and to show their relevance for turbulent flows, statistical data from corresponding three-dimensional DNS are provided wherever necessary.

Bearing in mind the above short review on the various research activities in turbulent premixed combustion, in the following a more detailed review

of some articles related to the present work by their ideas, methods or contents is given.

In [27] it is found that the local displacement flame speed as well as the normalized reaction term at the flame front are strongly dependent on the sign of the curvature: positive curvature, defined as flame front convex towards the fresh gases, has an almost negligible influence on the above parameters while negative curvature enhances them quite strong, although still linearly. In view of our further analysis it should be noticed that in [27] stoichiometric methane flames preheated to 800 K have been studied. In a similar earlier study of the same authors [28], it has been observed that highly diffusive and fast reactive species, H and H_2 , are well correlated with curvature, while CO, which is less diffusive and has a slow oxidation rate, is more susceptible to unsteady strain effects. Both [27] and [28] are two-dimensional studies of decaying turbulence and the initial turbulent field is prescribed by a two-dimensional turbulent kinetic energy spectrum function. Results therefore are statistically evaluated along the flame front at different time instances. In [29], together with the stoichiometric methane flame, a lean methane flame is studied. It is found that the displacement speed of the stoichiometric flame depends stronger on curvature in comparison with the lean flame. The fuel reaction rate shows strong correlation with negative curvature for both flames. A correlation between positive curvature and normal diffusion (one of the terms that contributes to the displacement speed of the premixed flame) is also found.

In another two-dimensional DNS study [30], the focus is set on the Lewis number effects. For this purpose three lean turbulent flames are simulated – a methane, a hydrogen and a propane flame having widely varying fuel Lewis numbers (Le). All computations are performed at turbulence conditions similar to those in laboratory-scale experiments and are performed using detailed chemical kinetics and transport properties. The statistical dependence of the consumption flame speed on curvature is presented for the three flames studied. The propane flame shows a clear negative correlation of the speed with curvature - flame speed is enhanced in regions of negative curvature indicating a thermo-diffusively stable flame. For the methane flame, the correlation is similar but much weaker, while the picture for the hydrogen flame is considerably different. For the hydrogen flame, there is a very strong positive correlation for positive curvature and a weaker positive correlation for negative curvature indicating that the flame is thermo-diffusively unstable, cf. also [16]. Local extinction of the hydrogen flame is observed in [30] at locations of negative curvature.

In [22] a two-dimensional DNS of methane flame at three different stoichiometric conditions (equivalence ratios $\Phi = 1.0, 0.75$ and 0.55) is performed with a detailed chemical kinetic mechanism (GRI-Mech 3.0). The results show that the flames react differently to curvature, depending on their equivalence ratio: the fuel consumption increases in areas of negative curvature for the flames with $\Phi = 1.0$ and 0.75 , while in the same areas it decreases for the flame with $\Phi = 0.55$. Because in [22] a mixture-averaged diffusive transport model is used, the different reaction of the three flames to curvature cannot be attributed to the Le , but rather to the effect of the equivalence ratio. In both [30] and [22], the authors investigate the effect of curvature on the local burning speed, but do not give data on tangential strain rates. They state that “the effects of strain on speed-versus-stretch correlations were entirely explained by the correlation of strain with curvature”.

Dinkelacker et al. [31] analysed experimental data and noticed a strong influence of the Lewis number on the average reaction rate even for highly turbulent methane/hydrogen/air lean premixed flames. This observation contradicts with their earlier experimental observation [32] that for highly turbulent flames positive and negative curvatures are symmetrically distributed along the flame front and with the assumed linear dependence of the local reaction rate on the curvature. In order to resolve this contradiction, a physical explanation (picture) is proposed in [31], which goes back to the ideas of “leading edge concept” from Zel’dovich and Frank-Kamenskii [34]. This physical picture considers the combined effects of Lewis number and curvature. According to it, the processes on the leading side of the flame (with mostly positive curvature towards the unburnt gases and for $Le < 1$) are assumed to be dominant for the flame propagation process and for the average reaction rate, while the rear side of the flame is assumed to have a minor importance. This picture practically abandons the assumption of linear dependence of local reaction rate on local curvature. Further, investigating hydrogen/methane/air flames, new definitions of effective Lewis number are proposed and used successfully in the modelling [31]. This model does not take into account tangential straining of the flames but includes normal diffusion across the flame front. The authors state that the paper discusses only the effects of curvature, but it is likely that both strain and curvature are important. They also discuss the necessity to adapt Markstein number models based on curvature in order to account for the observations leading to the physical picture proposed.

A systematic study of the Lewis number effects in two-dimensional turbulent premixed flames is carried out in [35]. Lewis numbers with values 0.8, 1.0 and 1.2 are simulated and it is found that local flamelets with $Le = 1$ are everywhere close to the undisturbed laminar flame. For $Le \neq 1$ a strong correlation with curvature is found and it is concluded that curvature is more important than strain rate in determining the local flame structure. However, tangential strain rate is found to be more important for the mean consumption rate per unit area of the flame and hence, for the turbulent flame speed. The tangential strain rate strongly depends on the Lewis number.

The literature review on the topic shows numerous investigations focused on determining specific parameters of premixed flames using different methodologies. However, for the correct physical understanding of the turbulent flame structure simultaneous availability of both statistical and local data for the same fuel and equivalence ratio are required. Therefore, the main objective of the present paper is to provide the reader with this kind of conflated information for different Lewis numbers. A second objective is to investigate the flame front non-homogeneities and the emerging of local extinction in case of extremely high or low Lewis numbers. Finally, the paper aims at demonstrating how a combination of fuels can be used to increase the flame homogeneity and to decrease the flame front sensitivity to the effects of curvature and strain.

To fulfil the above targets, the present paper considers the influence of the fuel’s Lewis number on the local heat release rate (HEATR). Both three-dimensional turbulence and two-dimensional flame-vortex interactions of premixed flames are investigated. The three-dimensional turbulence provides the necessary statistical data while the flame-vortex interactions serve to bring physical understanding of the local flame front processes. Detailed description of chemistry and transport data of the gas mixture is used without simplifying assumptions. The investigation is carried out for fuels with different Le and equivalence ratios. To compare the various simulated cases, a new index is introduced in §3.4.1 which quantifies the local inhomogeneity of the HEATR on the flame front. In order to find out the influence of extreme deviations of Le from 1.0 on the local extinction of the flame front, special numerical cases are designed in §3.5.1. Based on the newly acquired findings, the present work shows that fuels with $Le > 1$ can be mixed with fuels of $Le < 1$ to successfully enhance the homogeneity of the burning process along the flame front.

2. Methodology and Numerical Details

2.1 The Numerical Code and the Reaction Mechanisms

The fully compressible three-dimensional parallel version of the code PARCOMB [36] is used. The coupled system of the Navier-Stokes-, species- and energy conservation equations is solved. The resolution in space has an accuracy of sixth order and that in time – fourth order. The species transport data are simulated in detail (a complete multi-component diffusion treatment is applied) and the Soret effect is accounted for.

The hydrogen/air flame is modelled applying appropriately modified version of the H_2/O_2 sub-model described in [37]. The methane/air flame calculations are carried out with an in-house model, which is based on the reduced methane air chemical kinetic mechanisms presented in [38, 39 and 40]. The propane oxidation is modelled with a slightly modified version of the kinetic scheme called “M5 mechanism” adopted from [41 and 42], neglecting the NO_x chemistry described in [41]. In this mechanism, the rate coefficients of three pressure dependent reactions had to be reconsidered using [43] or best fit for the experimentally obtained pressure of 1 bar [16]. Due to the lack of data on the complete sets of thermodynamic and transport properties of the chosen kinetic scheme relevant data sets are adopted from [44]. This choice is made on the fact that, the original propane oxidation mechanism [41 and 42] is based on an earlier version of the chemical kinetic model [44], even though significantly reduced.

2.2 Computational Domain, Boundary and Initial Conditions

The three-dimensional computational domain spans $8 \times 5 \times 5$ [mm] and the numerical grid consists of $240 \times 150 \times 150$ equally distributed points. This ensures that the flame front of the flames listed in Table 1 is resolved by 14 to 28 numerical points. For the two-dimensional cases, the same resolution is kept for consistency. Along the x-axis, inflow and outflow conditions with Navier-Stokes characteristic boundary conditions are applied.

Table 1

One-dimensional flame calculations

Flame type	Φ	S_f [cm/s]	δ [mm]
H_2 /air	0.33	15.8	0.91
CH_4 /air	0.67	33.9	0.46
C_3H_8 /air	0.71	21.4	0.62

In each two-dimensional case, the laminar planar one-dimensional freely propagating flame is computed first. The one-dimensional result is copied along the y-axis and then a potential vortex is added to the velocity distribution. The result is shown in Fig. 1. The arrow shows the inflow of fresh gases. The domain boundaries along the y-axis (and the z-axes in the three-dimensional simulations) are periodic.

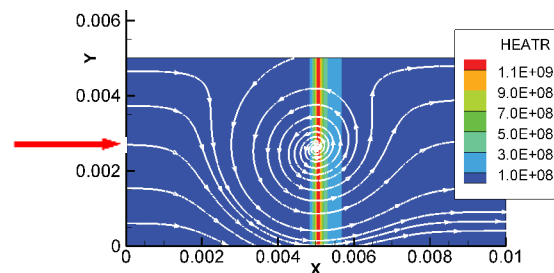


Fig. 1. Heat release rate (HEATR) in $[J/(m^3 \cdot s)]$ of the planar flame and initial streamlines (time instant $t = 0$) used for the flame-vortex interaction.

The potential vortex, which is used as initial condition in all two-dimensional simulations, is defined with its stream function ψ according to the following equation:

$$\Psi = \Gamma \cdot \text{EXP} \left(-0.5 \cdot \frac{\text{dist}^2}{r_{\text{vortex}}^2} \right)$$

In this equation the vortex strength (vorticity) is $\Gamma = 0.005$ [m^2/s], the radius of the vortex is $r_{\text{vortex}} = 0.0012$ [m] and dist [m] is the distance from the vortex origin to the corresponding points in the computational domain.

The vortices in the three-dimensional computation are initially zero and develop during the simulations from forcing in the physical domain. The interested reader is referred to [33] for more details.

2.3 Lewis and Markstein Numbers of the Investigated Fuels

The Lewis number is defined as $Le_i = a_{\text{MIX}}/D_i$, where “ a_{MIX} ” is the thermal diffusivity of the mixture [m^2/s] and “ D_i ” is the mass diffusivity of the chemical species “ i ” (in our case this is usually the fuel) into the mixture, [m^2/s].

The fuels studied are hydrogen, methane and propane air mixtures having Le ranging from small values ($Le_{H_2} = 0.29$) through values close to unity ($Le_{CH_4} = 0.97$) up to values higher than unity ($Le_{C_3H_8} = 1.81$). All numbers (except explicitly stated differently) are taken from [45] for stoichiometric propane combustion.

In the present study, experimentally determined Markstein numbers for the fuels of interest are taken from [46] and [17]. From these sources, for the methane/air flame the values for the Markstein number are $Ma \approx -2.0$ ($\Phi = 0.55$) and $Ma \approx 0.0$ ($\Phi = 0.67$). For the propane/air flame $Ma \approx 5.0$ ($\Phi = 0.71$) and for the hydrogen/air flame $Ma \approx -0.4$ ($\Phi = 0.33$). The negative values indicate that the flame is thermo-diffusively unstable, and vice-versa.

2.4 The Size of the Computational Domain and the Periodic Boundary Conditions

The size of the two-dimensional computational domain is intentionally chosen to be relatively small in order to allow quick repeating simulations with a large number of varying parameters. The influence of the size of the computational domain together with the imposed periodic boundary conditions on the shape of the curved and strained flame is presented on Fig. 2. The domain shown in this Figure is three times larger than the one used in the remaining simulations, which cover the area between the two dashed lines. Figure 2 is towards the end of the simulation, where the influence of the size of the domain is the largest. The physical time in Fig. 2 is a bit larger than the time in Fig. 3. The comparison of the two figures shows that the smaller domain size leads to locally increased values of the curvature, as it would be the case when interacting turbulent vortices are considered. However, the overall flame front shape and the levels of the heat release rate are quite similar. Therefore, the obtained results are generally representative of the flame-vortex interactions and the knowledge gained could be transferred to the more general case of turbulent flames.

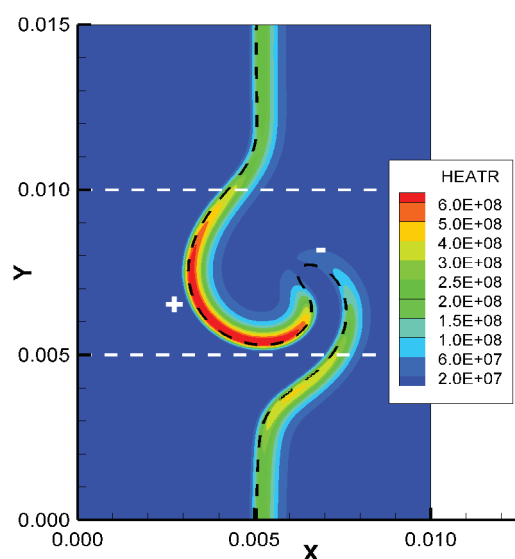


Fig. 2. HEATR, $\Phi_{(H_2/air)} = 0.33$, $t = 1.54$ [ms]. The location of the flame front is presented by the black dash line.

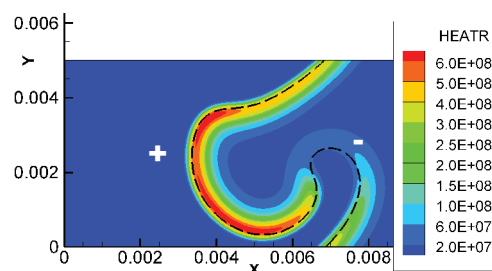


Fig. 3. HEATR, $\Phi_{(H_2/air)} = 0.33$, $t = 1.45$ [ms].

3. Results and Discussion

For the two-dimensional simulations, the flame front in this work is defined as the iso-surface of oxygen, which corresponds to 10% of the fresh gas fuel mass fraction. The corresponding values are extracted from the one-dimensional simulations. The statistical data for the three-dimensional computations are directly collected on the iso-surface, where the fuel mass fraction equals to 10% of the fresh gases mass fraction.

The HEATR is taken as a measure for the local response of the flame front to curvature and tangential strain rate. Its dimension in the figures is $[J/(m^3 \cdot s)]$. The curvature, which is convex towards the fresh gases, is defined as positive and vice versa; this definition is consistent with the literature [29, 30]. To support the reader, the sign of the curvature is presented in Fig. 4 and in all consequent figures.

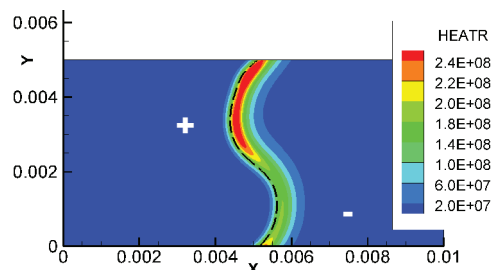


Fig. 4. HEATR, $\Phi_{(H_2/air)} = 0.33$, $t = 0.27$ [ms].

3.1 Results for Planar Non-Stretched Laminar Flames of Different Fuels

One-dimensional freely propagating, non-stretched (planar) laminar flame calculations are performed for H_2/air , CH_4/air and C_3H_8/air mixtures at lean combustion conditions (Table 1). The calculations are obtained using CHEMKIN PRO code [47] at pressure of one bar, unburnt gas temperature of 300 K and automatically estimated temperature profiles approved by the gas-phase equilibrium calculations. The freely propagating 1D-flame calculations are performed with the same reduced chemical kinetic mechanisms used for the 2D- and 3D-calculations.

lations, with a sufficient grid refinement achieving grid independent solution.

The simulated unstretched (planar) laminar flame speed, flame thickness and maximal net heat production from the gas-phase reactions are presented in Table 1. The flame thickness is defined as the ratio of the temperature difference between fresh and burnt gases (adiabatic temperature) and the maximum temperature gradient of the one-dimensional unstretched (planar) flame.

3.2 Review of the Flame Response to Non-Stationary Two-Dimensional Pure Straining

In the present section, the relative impact of pure straining is discussed. Curvature and tangential strain rate are often regarded together, because both contribute to flame stretch, for details see [6, 48 and 49]. Another reason for the combined treatment of curvature and strain rate is that in turbulent flames they appear always together and are well correlated statistically [22]. This is the case also in the present simulations. A possible way to study the role of curvature and strain separately would be to consider simple problems, where only one of them is present as in [48]. In this work, an initially straight planar flame was subject to unsteady stretch (without curvature) through a linear Couette-flow velocity distribution. The results showed that local extinction is not achieved even at relatively high velocity of 150 [m/s] (at strain rate 15000 [s^{-1}]) in case of lean methane and hydrogen flames. These results are presented in [48] and initially have led to the conclusion that these flames are not very sensitive to strain. A similar conclusion was reported also in [50]. The authors investigated near-stoichiometric methane/air oppositely directed identical round jets and stated that “the scalar structure of the flame, and thereby the flame thickness, are insensitive to strain rate variations for these purely strained flames, and that these flames cannot be extinguished by straining alone”.

Based on the results in [48], an additional study of the pure straining is carried out. The preliminary results are summarized as follows. The three fuels with different Lewis numbers react in different ways to pure straining. The lean hydrogen/air flame increases its flame speed and heat release rate considerably and the temperature increases above the adiabatic flame temperature. The lean methane/air flame with $Le \sim 1.0$ remained insensitive to strain (consistently with the findings of [48] and [50]) and the lean propane/air flame decreased the intensity of the heat release rate and of the flame speed. All three flames needed a certain initial time (called reaction delay time) of the order of 0.05 to 0.10 [ms] to start responding to the strain rate. The latter shows why

the models, which are based on the instantaneous functional dependence of the flame speed with strain rate and curvature, cannot show perfect correlation.

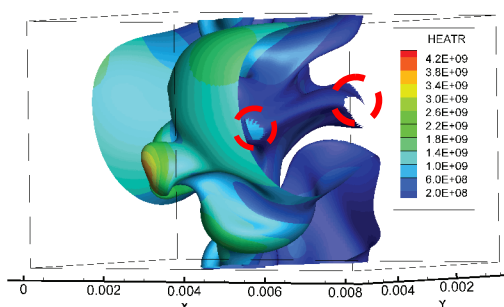
3.3 Statistical Data from Three-Dimensional Simulations (DNS) of Turbulent Lean Premixed Flames

In order to get an idea for the range of parameters further investigated, data originating from three-dimensional numerical simulations of lean turbulent premixed flames with the three fuels are presented in Table 2. The three-dimensional DNS investigate the flame response to a set of large-scale vortices. The method for generating the non-decaying vortices is described in detail in [48] and [33]. The vortex set is kept equal for all three simulations and the flame front for the hydrogen flame at time instant $t = 0.92$ [ms] is shown in Fig. 5. The vortices have an average length scale of 1.01 [mm] and the rms-value of the velocity fluctuations at $t = 0.92$ [ms] is between 2.05 and 2.32 [m/s]. Figure 5 shows that the local HEATR for the hydrogen flame is strongly amplified at the locations where the flame front is convex towards the fresh gases (the fresh gases enter the domain from the left hand side of the figure, i.e. at $x = 0.0$ [m]). For the hydrogen flame local extinction is present at locations where the curvature of the flame front has high values and is convex to the burnt gases (negative curvature). These locations are marked in red in the same figure.

The correlation coefficients between the HEATR and the curvature for all three fuels are quite high – the absolute values are above 0.68, see Table 2. It is important to note that the sign of the correlation coefficients for the three fuels differ, thus showing that the interdependence of HEATR and curvature for the methane and propane is opposite to hydrogen. Thus, in contrast to the hydrogen flame, for methane and propane the high values of positive curvature will lead to a decrease of the heat release rate. The correlation between the tangential strain rate and the heat release rate is positive and for all fuels, it has a much smaller value than the one for the curvature. This smaller value shows that, the curvature plays the major role on controlling the HEATR. Further, the table shows that the prevailing part of the flame front area is convex towards the fresh gases thus having positive curvature. In the same table the values for the average curvature of the flame front, its minima and maxima are also given. These show that very high extreme values can be reached in both positive and negative directions. As it is shown later in §3.4.1., the extreme curvatures reached in the current two-dimensional simulations are more than an order of magnitude lower than those from Table 2.

Table 2Statistical data from three-dimensional direct numerical simulations at time instant $t = 0.92$ [ms]

Fuel and equivalence ratio	Average curvature [m ⁻¹]	Min curvature [m ⁻¹]	Max curvature [m ⁻¹]	Flame front area with positive curvature [%]	Correlation coefficients: curvature & HEATR, strain rate & HEATR
H ₂ , $\Phi = 0.33$	145	-13378	18895	60.01	0.683, 0.089
CH ₄ , $\Phi = 0.67$	-11	-9889	10371	57.1	-0.792, 0.396
C ₃ H ₈ , $\Phi = 0.71$	225	-10349	25910	56.5	-0.726, 0.208

Fig. 5. HEATR and local flame extinction $\Phi_{(H_2/air)} = 0.33$, at $t = 0.92$ [ms].

The present work focuses mainly on investigating the local functional dependences between the curvature and the HEATR at different Le numbers. Two-dimensional simulations allow therefore tracing and visualising the time development of parameters and their interdependence, overcoming the obstacles of processing and visualising of a large outcome from three-dimensional calculations with complex and wrinkled flame fronts. For this purpose, the following results are obtained and presented in two spatial dimensions, and current three-dimensional results will be recalled for comparison wherever appropriate for the discussion. Additional data about the setup and turbulence of the three-dimensional simulations are given in [33].

3.4. Flame front Response to Curvature in the Case of Pure Fuels with Different Lewis Numbers

3.4.1. Lean Hydrogen Flame, $\Phi = 0.33$

Figure 4 shows the HEATR for the hydrogen flame shortly after the beginning of the interaction with the vortex. Depending on the curvature, the flame front exhibits areas with enhanced HEATR and areas with strongly suppressed HEATR. The enhanced HEATR is observed at points, where the flame front has a positive curvature whereas the decreased HEATR is located at negative curvature. In this work, in consistence with [51], the behaviour

that splits the flame front into areas of relatively increased and decreased heat release rates is called “polarization effect”. It has been shown in [51] that radicals as OH, H or O also underlie the polarisation effect.

In the following, some data are presented in order to allow a comparison with the values from Table 2. The maximum curvature value at the flame front is 1093 m^{-1} and the minimum is -936 m^{-1} . The averaged heat release rate (over the number of points at the flame front) for this early time is $\text{HEATR} = 1.65\text{E}+08 \text{ J}/(\text{m}^3.\text{s})$ which is lower than the corresponding value of the planar unstrained flame: $\text{HEATR} = 2.12\text{E}+08 \text{ J}/(\text{m}^3.\text{s})$. For the points with positive curvature, it is expected to have a higher HEATR than the planar unstrained flame. However, against the expectations, the conditional average for all points with positive curvature is $\text{HEATR} = 1.82\text{E}+08 \text{ J}/(\text{m}^3.\text{s})$. The percentage of points on the flame front with positive curvature is 53.4%. The correlation coefficient between the curvature and the HEATR is equal to 0.68, i.e. this value is the same as for the three-dimensional simulation, c.f. Table 2.

A later time instant with increased flame front curvature is shown in Fig. 3. Here the polarisation effect is getting stronger. It is useful to quantify the maximum and the minimum of the HEATR at the flame front for this time instant: $t = 1.45$ [ms]. At the same time instant $\text{HEATR}_{\text{MAX}} = 5.63\text{E}+08 \text{ J}/(\text{m}^3.\text{s})$ and $\text{HEATR}_{\text{MIN}} = 2.23\text{E}+07 \text{ J}/(\text{m}^3.\text{s})$. Therefore, their ratio:

$$PEN = \frac{\text{HEATR}_{\text{MAX}}}{\text{HEATR}_{\text{MIN}}}\bigg|_{\text{FLAME_FRONT}}$$

could be defined as a measure for the above mentioned polarisation effect. The ratio defined by equation (1) will be called further the “Polarisation Effect Number” (PEN). The closer the PEN is to the value of 1.0, the smaller the combined effect of curvature and strain is. Large values of PEN show large influence of curvature, which effect is observed when

the Le for the deficient reactant deviates considerably from unity. Thus, the PEN is just a number that quantifies the combined effects resulting from curvature, strain rate and Lewis number of the deficient reactant. It presents a local quantity that expresses the magnitude of the polarization effect of a local vortex. However, the PEN does not present a new physical effect and therefore it should not be used to explain the observed polarisation.

In Fig. 3, the PEN value equals to 25.3. The maximum curvature is $1381 \text{ [m}^{-1}\text{]}$ while the minimum is $-2661 \text{ [m}^{-1}\text{]}$ whereas the maximum tangential strain rate is $1389 \text{ [s}^{-1}\text{]}$ and the minimum is $-116 \text{ [s}^{-1}\text{]}$. At later time steps, the strong negative curvature leads even to local extinction of the flame.

At the time instant $t = 1.45 \text{ [ms]}$ the average HEATR = $3.59\text{E}+08 \text{ [J/(m}^3\text{.s)]}$ is much higher than that for the unstrained planar flame given above. This is true for the conditional average of both positive and negative curvature: for the points with positive curvature, the value is HEATR = $4.83\text{E}+08 \text{ [J/(m}^3\text{.s)]}$ while for the points with negative curvature - HEATR = $2.35\text{E}+08 \text{ [J/(m}^3\text{.s)]}$. Note that against the expectations, the latter value is higher than that of the unstrained planar flame but that such effect is not observed for the lean hydrocarbon fuels. The percentage of points with positive curvature is 50.2% and the correlation coefficient between the curvature and the HEATR is 0.76.

With the last values of the heat release rate one can see that even the negatively curved regions of the flame contribute quite a lot to the enhancement of the reaction rate. Therefore, at least for this particular fuel and flame-vortex interaction, the physical picture of [31] which neglects the contribution of negatively curved regions on the reaction rate, needs some revision.

3.4.2. Lean Methane Flames, $\Phi = 0.67$ and $\Phi = 0.55$

Unlike the hydrogen flame, the lean methane flame ($\Phi = 0.67$) burns with an almost constant HEATR along the complete flame front. For this Lewis number ($Le \approx 1$) the flame is almost unaffected by curvature (Fig. 6). The polarisation effect number here has a value 1.06.

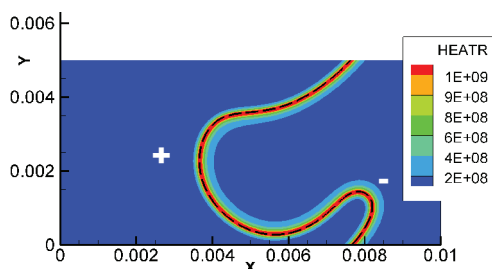


Fig. 6. HEATR, $\Phi_{(CH_4/air)} = 0.67$, $t = 1.43 \text{ [ms]}$.

For comparison, a computation is made with methane fuel but with an equivalence ratio $\Phi = 0.55$. For the time instant $t = 1.3 \text{ [ms]}$ the result is shown in Fig. 7. The homogeneity of the HEATR at the flame front here is a bit less than that for the higher equivalence ratio (here PEN = 1.18). Both Figs. 6 and 7 reveal that the behaviour of the flame corresponds to the Markstein number from §2.3. The richer flame, according to $Ma = 0.0$, does not react to curvature or strain. At the same time, the leaner flame with $Ma = -2.0$, behaves similar to the hydrogen flame for which Markstein number is also negative.

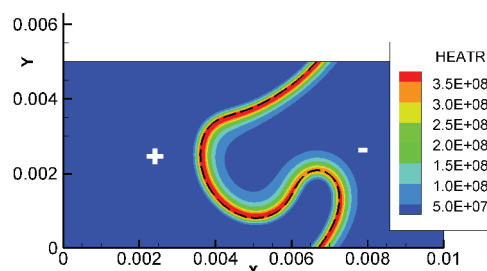


Fig. 7. HEATR, $\Phi_{(CH_4/air)} = 0.55$, $t = 1.3 \text{ [ms]}$.

The equivalence ratio changes the mixture properties and consequently the Le of the species as well. Initially, it seemed not clear whether the increased polarisation for $\Phi = 0.55$ should be attributed only to Le , or both equivalence ratio and Le . In a similar study [22], the Le is kept constant and the equivalence ratio is varied. The results in [22] show that the flame structure depends on the equivalence ratio. In order to investigate in detail the question of whether the Le number or the equivalence ratio are the real source for the differences, the present fuel Lewis numbers have been exactly calculated. For this purpose, the one-dimensional simulation of the unstrained planar flame was considered. The current results show that differences in the Lewis number are quite small: in the fresh gases $Le = 1.0469$ for $\Phi = 0.55$ and $Le = 1.0429$ for $\Phi = 0.67$, which means that the difference is less than 0.4%. At the high temperature region the Lewis number is $\Phi = 0.55$ for $Le = 0.848$ and $Le = 0.847$ for $\Phi = 0.67$, which is less than 0.2% difference. These results lead to the conclusion that the observed differences in the PEN for the two equivalence ratios cannot be attributed only to the differences in the Lewis number. The observed influence of Φ on the flame structure suggests that the different stoichiometry is associated with the variation in the rate limiting reaction pathways and the dominance of different species and their diffusion near the flame front. Thus, the adiabatic flame temperature also considerably differs (1575 K for $\Phi = 0.55$ and 1788 K for $\Phi = 0.67$). All these considerations propose possible explanation for the different PEN in Figs. 6 and 7.

3.4.3. Lean Propane Flame, $\Phi = 0.71$

The lean propane flame, which has $Le > 1$, behaves exactly opposite to the hydrogen flame: the HEATR increases in areas of negative curvature, while it decreases in areas of positive curvature as shown in Fig. 8. The PEN here is 4.1. However, even at higher curvatures, the polarisation effect for this propane flame is not sufficient to allow local extinction.

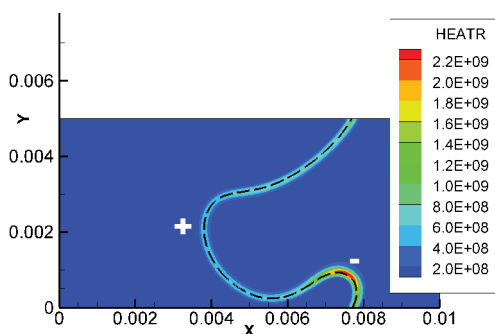


Fig. 8. HEATR, $\Phi_{(C_3H_8/air)} = 0.71$, $t = 1.63$ [ms].

3.4.4 Rich Hydrogen Flame, $\Phi = 6.0$

The heat release rate at a flame-vortex interaction in case of rich hydrogen flame is given in Fig. 9. Here the deficient reactant is the oxygen which Lewis number is larger than 1.0. At the same time, the fuel Le number presented in [52] is 2.2. Therefore, it is expected that this rich flame will have different response to curvature than the lean hydrogen flame. Indeed, the heat release rate for the negatively curved parts of the flame front is amplified, and vice-versa. This is exactly opposite to the observations in Fig. 4 for the lean flame.

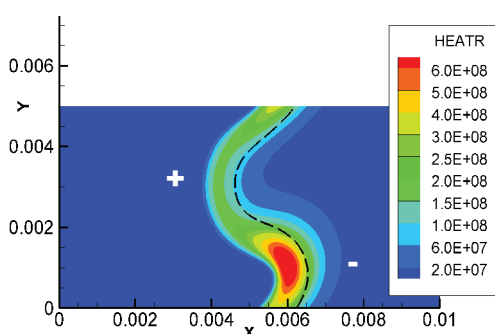


Fig. 9. HEATR, $\Phi_{(H_2/air)} = 6.0$, $t = 0.64$ [ms].

The value of PEN in Fig. 9 is 3.44. The flame front here is defined differently than in the lean cases: the isoline is based on the oxygen, which corresponds to 10% from the oxygen mass fraction in the unburned

gases. It can be seen that the current definition shifts the flame front towards the right hand side of the maximum heat release rate, which finally leads to an underprediction of the PEN value. Indeed, if the absolute maximum and minimum HEATR along the relatively thick flame front is taken into account, the value of PEN increases and becomes $PEN = 5.04$.

It is important to notice that this rich flame shows higher polarization at later time instances which finally leads to its extinction at the location of positive curvature.

3.5. Controlling the Heat Release Rate Homogeneity by Means of Varying the Lewis Numbers

The next investigations present the use of Le for controlling the behaviour of the flame. First, two examples with a single fuel with extremely large or small Le are shown. Then, a combination of two fuels (hydrogen with $Le < 1$ and propane with $Le > 1$) is simulated showing that it is possible to obtain a mixture of fuels with a low number of PEN.

3.5.1. Artificially Changed Lewis Numbers of the Methane Flame to Achieve Different Polarisation Effects

As shown in §3.4.2 the methane flame with $\Phi = 0.67$ has almost no polarisation effect. Therefore, the same case is studied in the two following examples. The main idea is to vary strongly only the diffusion coefficient of the fuel into the mixture, i.e. the Le of the fuel, in order to see the influence of this parameter on the polarisation effect. Furthermore, it is important to examine whether the variation of Le will lead also to local flame extinction.

In the first simulation, after the exact computation of the diffusion coefficient of methane into the mixture, the value is artificially multiplied by 10. This way the Le of the fuel is decreased 10 times and now, the methane should resemble the flame response to curvature, which is typical for hydrogen. The result is presented in Fig. 10.

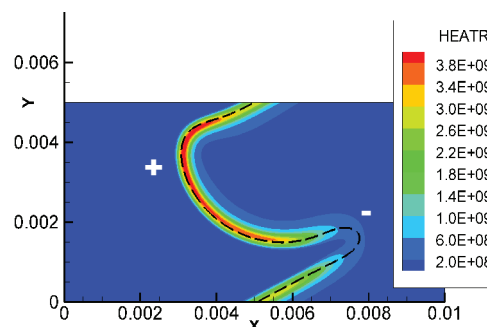


Fig. 10. HEATR, $\Phi_{(CH_4/air)} = 0.67$, $t = 1.01$ [ms], CH_4 – flame with 10 times increased diffusion coefficient.

Figure 10 shows that indeed the methane flame with the modified diffusion coefficient acquires the quality of the hydrogen flame: the HEATR increases in regions of positive curvature and decreases strongly in regions of negative curvature up to the point of extinguishing.

As expected, the small value of the Lewis number ($Le \approx 0.1$) leads to larger PEN. It is worth comparing this case with the hydrogen flame ($Le = 0.29$). The polarisation effect number for the flame in Fig. 10 is $PEN = 14.5$, while for the same time instant ($t = 1.01$ [ms]) the hydrogen flame has a lower value - $PEN = 11.2$.

In order to complete the investigation, also a simulation with 10 times decreased diffusion coefficient of methane into the mixture has been carried out. The result is shown in Fig. 11. The qualitative behaviour is now similar to that of the propane flame; however, due to the much lower diffusion coefficient the present flame clearly shows local extinction. The polarisation effect number here is $PEN = 23.6$.

It is proven here, that by simply changing the diffusion coefficient of methane into the mixture the flame response to curvature as well as the local extinguishing of the flame depends to quite a large extent on the Lewis number.

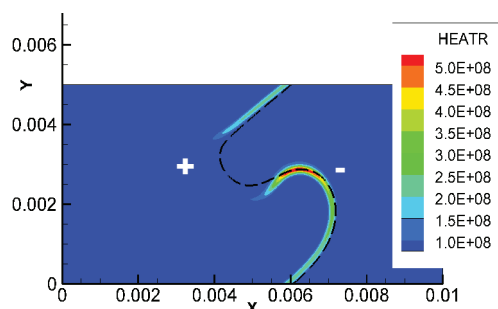


Fig. 11. HEATR, $\Phi_{(CH_4/air)} = 0.67$, $t = 1.01$ [ms], CH_4 - flame with 10 times decreased diffusion coefficient

3.5.2. A Mixture of Two Fuels with Lewis Numbers Smaller and Larger than 1.0

Here, on the example of the propane mechanism, a mixture of hydrogen and propane is taken, in order to show that through appropriate proportion the polarisation effect can be largely controlled. This way, indirectly (through controlling the polarisation effect) the local extinguishing is also controlled and could be avoided. The main idea for studying a fuel mixture is that the effects of polarisation will cancel out for the two fuels (due to their different response to positive and negative curvature), thus leading to an almost homogeneous distribution of the HEATR at the flame front.

First, a mixture of hydrogen and propane is considered for which the mass fractions of the fresh gases are given in Table 3. In all three cases, the mixture is lean.

The results for case 1 show that the mixture behaves similarly to the hydrogen flame and at this early time instant it has a relatively large PEN ($PEN = 2.86$). As a next step, the fuel mass fractions are increased twice (case 2, Table 3). The result for the HEATR at the same time instant for case 2 is presented in Fig. 12. The heat release rate is now almost evenly distributed along the flame front, at both positive and negative curvatures. Here the $PEN = 1.27$ and the minimum HEATR appears at the straight part of the flame front (the non-curved part appears near the periodic boundaries of the domain). This minimum is 13% lower than the maximum HEATR of the non-stretched planar flame. For case 2, the positive curvature still exhibits a large HEATR, which manifests stronger at later time instances. Therefore, in order to increase more the homogeneity of the HEATR the mass fraction of the fuel with larger Le (propane) should be increased appropriately (see case 3).

Table 3

Mass fractions of the fresh gases for the simulated cases

Mass fraction	H ₂	C ₃ H ₈	O ₂	N ₂
Case 1	0.0026	0.0181	0.2310	0.7483
Case 2	0.0050	0.0360	0.2310	0.7280
Case 3	0.0050	0.0400	0.2310	0.7240

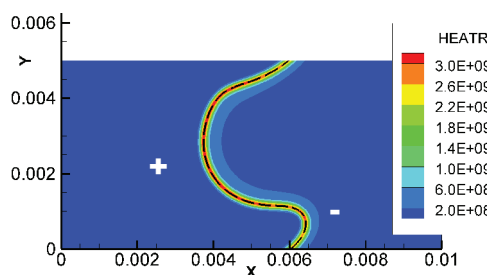


Fig. 12. HEATR, $t = 0.7$ [ms], H₂/C₃H₈ - flame, case 2.

For time instant $t = 0.7$ [ms], case 3, the HEATR at the location of highest positive curvature is equal to $4.37E+09$ [J/(m³.s)], and at the highest negative - $4.27E+09$ [J/(m³.s)]. The ratio of these two numbers is 1.02, but the PEN for the whole flame front is higher, $PEN = 1.21$, which can be interpreted from the results shown in Fig. 13. The minimum of the HEATR in Fig. 13 appears near the inflection points of the flame front (near almost straight parts of the flame

front or parts with small negative curvature). At later time instant, the PEN equals 1.50 with the smallest HEATR, appearing again at locations of small or vanishing value of the curvature. Obviously, at these locations straining of the flame front is responsible for the lowest heat release rates, which values are below those for the non-stretched planar flame.

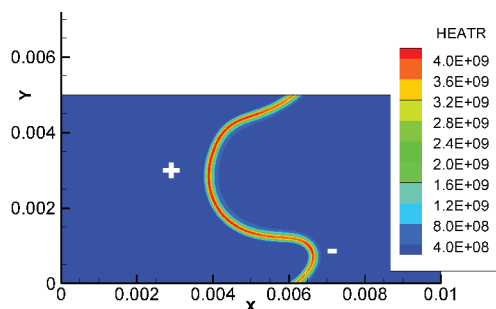


Fig. 13. HEATR, $t = 0.7$ [ms], $\text{H}_2/\text{C}_3\text{H}_8$ – flame, case 3.

4. Conclusions

Results from three-dimensional Direct Numerical Simulations as well as from two-dimensional flame-vortex interactions are presented and discussed. The methodology uses detailed (or semi-detailed) chemical kinetic mechanisms together with detailed computation of all mixture transport properties. The response of fuels with different Lewis number to flame front curvature and strain rate is studied statistically and locally. The fuels investigated comprise lean hydrogen ($Le < 1$), rich hydrogen ($Le > 1$), lean methane ($Le \approx 1$) and lean propane ($Le > 1$). The results have been discussed in terms of both local (heat release rate, homogeneity, local extinction) and global (statistical) parameters. The investigated examples for the influence of the Le on the flame-vortex interaction can be used for the development of new phenomenological models of turbulent flames.

Three-dimensional DNS of lean premixed turbulent combustion showed a high statistical correlation between the curvature of the flame front and the local heat release rate: for all three lean flames the absolute value of the correlation coefficient was higher than 0.68. The statistical correlation of the HEATR and the tangential strain rate is found to be relatively small, but always positive. Very high extreme values of curvature are observed in the three-dimensional simulations, which are more than one order of magnitude higher than the corresponding two-dimensional simulations.

Important effect of the presence of large-scale vortices is the bending of the flame front. As a re-

sult, both positive and negative curvatures of the flame front occur simultaneously. In this case, near a vortex, the flame responds with a twofold change in the heat release rate: enhancement and decrease. This effect, resulting from the flame-vortex interaction, is called “polarisation effect”. For the quantification of this effect, a local criterion called PEN (Polarisation Effect Number, §3.4.1) has been introduced. It shows the inhomogeneity of the HEATR at the flame front. As expected, for fuels with Le number close to 1.0, the HEATR is quite homogeneous and the values of PEN are close to 1.0. The lowest values of PEN are found for the lean methane flame with equivalence ratio 0.67. The more the Le number of a fuel deviates from 1.0, the PEN value increases and for very high PEN numbers even local extinction is observed.

The impact of Lewis numbers much different than 1.0 on the local structure of the flame front has been investigated. The very lean hydrogen flame with $Le = 0.29$ showed high inhomogeneity and local extinction at times larger than 1.4 milliseconds for locations with negative curvature (flame front curved towards the burnt gases). The rich hydrogen flame with $Le_{\text{H}_2} = 2.2$ showed also a high value of PEN but local extinction at locations of positive curvature. These results inspired the design of two additional cases with $Le = 0.1$ and $Le = 10.0$. These two cases were created artificially: starting from the methane flame with the highest homogeneity ($Le \approx 1.0$, $\Phi = 0.67$ and PEN close to 1.0) the diffusion coefficient of methane was multiplied/divided by 10. The results show, that for these extreme Lewis numbers PEN values increase (when compared to the corresponding hydrogen flames) and local extinction emerges relatively early, approximately at $t = 1.0$ [ms].

Generally, local extinction has been found even for the thermodynamically stable flames when the Lewis number is much higher than 1.0. Such extinction is observed in both, the rich hydrogen flame with $Le_{\text{H}_2} = 2.2$ and the artificially designed case with methane diffusion increased to reach $Le \approx 10.0$.

Flames which fuel has a Le around unity are almost insensitive to curvature and their heat release rate remains almost constant along the flame front. In this case, slight variations in the qualitative and quantitative response to curvature and strain rate are possible when the equivalence ratio is varied, as this has been shown for the lean methane flame.

When two fuels of $Le < 1$ (lean hydrogen) and $Le > 1$ (lean propane) are mixed together, it is possible to obtain a lean fuel mixture which shows increased homogeneity of the flame front, i.e. having

low values of PEN. Therefore, such fuels are also relatively resistant to local extinction of the flame front.

Future perspectives of the present work envisage the development of analytical expressions for the PEN as a function of the Le , of the maximum and minimum curvatures of the flame front, and eventually – of the equivalence ratio for different fuels in the case of premixed combustion.

Acknowledgments

The authors would like to thank the High Performance Computing Centre Stuttgart (HLRS) for the provision of computer time on CRAY-XE6 under the grant “DNSPREM”. The financial support of DFG Special Priority Programme 606, Subproject B8 is kindly appreciated.

References

- [1]. G.H. Markstein, Nonsteady flame propagation, AGARD Monograph No. 75, Pergamon Press, New York, 1964.
- [2]. F.A. Williams. Combustion theory. Benjamin Cummings, Menlo park, CA, 1985.
- [3]. S.M. Candel and T.J. Poinso, Combust. Sci. and Tech. 70 (1990) 1–15.
- [4]. R.S. Cant and E. Mastorakos, An introduction to turbulent reacting flows, Imperial College Press, 2008.
- [5]. P. Clavin, Prog. Energy Combust. Sci. 11 (1985) 1–59.
- [6]. P. Poinso and D. Veynante, Theoretical and numerical combustion, Second edition, Edwards, 2005.
- [7]. C.K. Law, D.L. Zhu, and G. Yu, Proc. Comb. Inst. 21 (1986) 1419–1426.
- [8]. C.J. Sung, J.B. Liu and C.K. Law, Combust. Flame 106 (1996) 168–183.
- [9]. C.K. Law, Proc. Comb. Inst. 22 (1988) 1381–1402.
- [10]. J. Sato, Proc. Comb. Inst. 9 (1982) 1541–1548.
- [11]. H.G. Im and J.H. Chen, Proc. Comb. Inst. 28 (2000) 1833-1840.
- [12]. C. Schrödinger, C.O. Pashereit, and M. Oevermann, ICCFD7-3401, Hawaii, July 9-13, 2012.
- [13]. H.G. Im, J.H. Chen and J.Y. Chen, Combust. Flame 118 (1999) 204–212.
- [14]. M. Weiß, N. Zarzalis and R. Suntz, Combust. Flame 154 (2008) 671–691.
- [15]. P. Clavin and J.C. Grana-Otero, J. Fluid Mech. 686 (2011) 187–217.
- [16]. J.A. Denev, V. Vukadinovic, I. Naydenova, N. Zarzalis and H. Bockhorn, Proceedings of the European Combustion Meeting, Lund, 26-28th of June, publ. No: P1-69, 6p, 2013.
- [17]. K.T. Aung, M.I. Hassan and G.M. Faeth, Combust. Flame 109 (1997) 1–24.
- [18]. O.C. Kwon, and G. M. Faeth, Combust. Flame 124 (2001) 590–610.
- [19]. M. Weiss, Untersuchungen von Flammenfrontstreckungseffekten auf die sphärische Flammenausbreitung laminarer und turbulenter Brennstoff/Luft-Gemische, Ph.D. Thesis, University of Karlsruhe, 2008, in German.
- [20]. N. Peters, Turbulent combustion, Cambridge University Press, 2000.
- [21]. D. Bradley, Proc. Combust. Inst. 24 (1992) 247–262.
- [22]. J.B. Bell, M.S. Day, J.F. Grcar, and M.J. Lijewski, Commun. App. Math. Comput. Sci., 1, Mathematical Sciences Publishers, p. 29–52, 2006.
- [23]. R. Borghi, in C. Casci (ed.), Recent advances in aerospace sciences, Plenum, New York, 1985, 117-138.
- [24]. K.K. Kuo and R. Acharya, Fundamentals of turbulent and multiphase combustion, John Wiley and Sons, Inc., 2012.
- [25]. A.M. Laverdant, and S.M. Candel, Combust. Sci. and Tech. 60 (1988) 79–96.
- [26]. W.T. Ashurst and P.A. McMurtry, Combust. Sci. and Tech. 66 (1989) 17–37.
- [27]. T. Echekki and J.H. Chen, Combust. Flame 118 (1999) 308–311.
- [28]. T. Echekki and J.H. Chen, Combust. Flame 106 (1996) 184–202.
- [29]. N. Peters, P. Terhoeven, J.H. Chen and T. Echekki, Proc. Comb. Inst. 27 (1998) 833–839.
- [30]. J.B. Bell, R.K. Cheng, M.S. Day and I.G. Shepherd. Proc. Comb. Inst. 31 (2007) 1309–1317.
- [31]. F. Dinkelacker, B. Manickam, and S.P.R. Muppala. Combust. Flame 158 (2011) 1742–1749.
- [32]. A. Soika, F. Dinkelacker and A. Leipertz, Combust. Flame 132 (2003) 451–462.
- [33]. J.A. Denev and H. Bockhorn, Accepted in Transactions of the High Performance Computing Center, Stuttgart (HLRS), Springer, (2014).
- [34]. Y.B. Zel’dovich and D.A. Frank-Kamenteskii, Turbulent and Heterogeneous Combustion, MMI, Moscow, 1947 (in Russian).
- [35]. D.C. Haworth and T.J. Poinso, J. Fluid Mech., 244 (1992) 405–436.
- [36]. D. Thevenin, F. Behrendt, U. Maas, B.

- Przywara and J. Warnatz, *Computers and Fluids* 25 (1996) 485–496.
- [37]. J.A. Miller, R.E. Mitchell, M.D. Smooke and R.J. Kee, *Proc. Comb. Inst.* 19 (1982) 181–196.
- [38]. R.W. Bilger, M.B. Esler and S.H. Starner, In: *Reduced Kinetic Mechanisms and Asymptotic Approximations for Methane-Air Flames Lecture Notes in Physics Volume*, (Ed.) M. D. Smooke, Springer Berlin Heidelberg, Springer-Verlag, 384, 1991, p. 86.
- [39]. M.D. Smooke and V. Giovangigli, In: *Reduced Kinetic Mechanisms and Asymptotic Approximations for Methane-Air Flames Lecture Notes in Physics Volume*, (Ed.) M. D. Smooke, Springer Berlin Heidelberg, Springer-Verlag, 384, 1991, p.1.
- [40]. M.D. Smooke and V. Giovangigli, In: *Reduced Kinetic Mechanisms and Asymptotic Approximations for Methane-Air Flames Lecture Notes in Physics Volume*, (Ed.) M. D. Smooke, Springer Berlin Heidelberg, Springer-Verlag, 384, 1991, p.29.
- [41]. C. Jimenez, B. Cuenot, T. Poinot, and Haworth, D., *Numerical Combust. Flame* 128 (1-2) (2002)1–21.
- [42]. D.C. Haworth, R.J. Blint, B. Cuenot and T.J. Poinot, *Combust. Flame* 121 (4) (2000) 395–417.
- [43]. D.L. Baulch, C.T. Bowman, C.J. Cobos, R.A. Cox, Th. Just, J.A. Kerr, M.J. Pilling, D. Stocker, J. Troe, W. Tsang, R.W. Walker and J. Warnatz, *J. Phys. Chem. Ref. Data.* 34 (2005) 757–1397.
- [44]. C.I. Heghes, C1-C4 Hydrocarbon oxidation mechanism, PhD thesis, Ruprecht-Karls-Heidelberg University, Heidelberg, Germany, 2006.
- [45]. B. Ranganath and T. Echehki, *Int. J. Heat Mass Transfer* 49 (25-26) (2006) 5075–5080.
- [46]. L.K. Tseng, M. Ismail and G. Faeth, *Combust. Flame* 95 (1993) 410-426.
- [47]. CHEMKIN-PRO Release 15 113, 2012.
- [48]. J.A. Denev and H. Bockhorn, in *Transactions of the High Performance Computing Center, Stuttgart (HLRS)*, Springer, (2013) p. 245–257.
- [49]. J.H. Chen and H.G. Im, *Proc. Comb. Inst.* 28 (2000) 211–218.
- [50]. C.K. Law, C.J. Sung, G. Yu and R.L. Axelbaum, *Combust. Flame* 98 (1995) 139–154.
- [51]. J.A. Denev and H. Bockhorn, In 26. *Deutscher Flammentag, Verbrennung und Feuerungen*, VDI-Berichte 2161, VDI, Duisburg-Essen, 11.-12. September, pp. 601-612, 2013.
- [52]. Z. Chen, M. Burke, and Y. Ju, *Proc. Comb. Inst.* 32 (2009) 1253–1260.

Received 20 March 2014